Quantum Beats and Chaos in the Hénon-Heiles Hamiltonian

M. Brack,[1],[2] R. K. Bhaduri,[1] J. Law,[1],[3] and M. V. N. Murthy[1],[4]
[1] *Department of Physics and Astronomy, McMaster University, Hamilton, Ontario, Canada L8S 4M1*
[2] *Institute for Theoretical Physics, University of Regensburg, D-8400 Regensburg, Germany*
[3] *Department of Physics, University of Guelph, Guelph, Ontario, Canada N1G 2W1*
[4] *Institute of Mathematical Sciences, Madras 600 113, India*
(Received 15 June 1992; revised manuscript received 8 October 1992)

The quantum density of states of the Hénon-Heiles Hamiltonian exhibits prominent low-frequency beats as a function of energy. We interpret the beats in terms of interferences of the three simplest isolated classical periodic orbits by a calculation of their amplitudes in the Gutzwiller trace formula. We show that periodic orbit theory can reproduce classically the main characteristics of the quantum beats. Both stable and unstable orbits contribute substantially in generating these long-range correlations, which coexist with the short-range fluctuations giving nearest-neighbor spacings distributions typical for chaos. With a Fourier analysis our conclusions confirm the quantum spectrum.

PACS numbers: 05.45.+b, 02.50.–r, 03.65.Ge

The quantal behavior of a system exhibiting classical chaos is of considerable interest [1, 2]. For a Hamiltonian system, it is customary to study the eigenspectrum in two complementary ways. The *local* behavior of the spectrum is typically analyzed by studying the distribution of nearest-neighbor spacings (NNS) [3]. In nonintegrable systems, this unfolds level repulsions which, through random matrix theory, are used as a test [4] for "quantum chaos." The *global* behavior of a spectrum is given by the quantum density of states as a function of energy [5, 6]. Its analysis unravels the long-range correlations in the energy spectrum, which often appear as oscillations. These oscillations are, through periodic orbit theory [1], related to the classical periodic orbits. Even a classically ergodic system may have isolated periodic orbits that give rise to strong Fourier amplitudes of the spectral density [7]. Typically, the orbits with the shortest time periods set the largest energy scales for the oscillations. If, however, a few of these orbits have close-by frequencies and amplitudes, beats may arise with modulated amplitudes on a much larger energy scale. Such beats were found in an integrable system by Balian and Bloch [8] in their investigation of the spectral density of a spherical cavity with reflecting walls. It is dominated by the interference of triangular and square trajectories. Metal clusters provide a physical many-body system, in which such beats occur in the form of "supershells" [9] and have experimentally been put into evidence [10].

In this paper, we demonstrate for the first time the existence of beats in a classically chaotic system, namely, the well-studied Hénon-Heiles potential [11]. We associate its quantum beats to the three primitive classical periodic orbits [12] of nearly equal frequencies and amplitudes.

The Hénon-Heiles Hamiltonian describes the planar motion of a single particle and is given by

$$H = \frac{1}{2}(p_x^2 + p_y^2) + \frac{1}{2}(x^2 + y^2) + \alpha\left(x^2 y - \frac{1}{3}y^3\right). \qquad (1)$$

Here α is a parameter governing the anharmonicity. By convention we set $\hbar = m = \omega = 1$. The quantum spectrum of this Hamiltonian has been examined by many groups [13]. Because of the noncentral nature of the potential, the angular momentum l is not a good quantum number. We diagonalize the Hamiltonian in a large harmonic oscillator basis $|n, l\rangle$ with radial quantum number n. The anharmonic term in H mixes states with $\Delta l = \pm 3$. Clearly, this mixing takes place in three disconnected sets of basis states: $\{a\}$ $l \in \{...-6, -3, 0, 3, 6...\}$, $\{b\}$ $l \in \{...-5, -2, 1, 4...\}$, and $\{c\}$ $l \in \{... - 4, -1, 2, 5...\}$. Each set has nondegenerate eigenvalues. Under time reversal, set $\{a\}$ maps onto itself, while $\{b\}$ maps onto $\{c\}$ and *vice versa*. Therefore, sets $\{b\}$ and $\{c\}$ have identical eigenspectra due to the time reversal symmetry of the Hamiltonian (1). Thus, H may be diagonalized in each basis set separately. For the global analysis of the spectrum, all three sets of eigenvalues are combined, whereas for an NNS distribution, the spectra of the different sets are examined individually.

It should be pointed out that in principle all the "bound states" for the Hamiltonian (1) have nonzero widths as the particle may tunnel out through the barriers. Along the three symmetry axes, the barrier height is minimum (see Fig. 1), and the classical escape (or saddle point) energy is $E^* = 1/6\alpha^2$. The eigenvalues represent the spectrum accurately if the true widths are small compared to the averaged level spacing. The discretized continuum approximately simulates the low-lying resonances [14]. We found that the energy eigenvalues immediately above E^* change only by less than a few percent of the average level spacing as the basis size is increased from a cutoff energy of $E_{\rm cut} = 66$ to $E_{\rm cut} = 101$.

An analysis of NNS distributions of the energy level set $\{b\}$ (or $\{c\}$) reveals that the system is transitional between regular and chaotic for $\alpha = 0.06$ and chaotic at $\alpha = 0.08$. (In order to have enough statistics, we could only go up to $\alpha = 0.08$ in calculating the NNS distributions.)

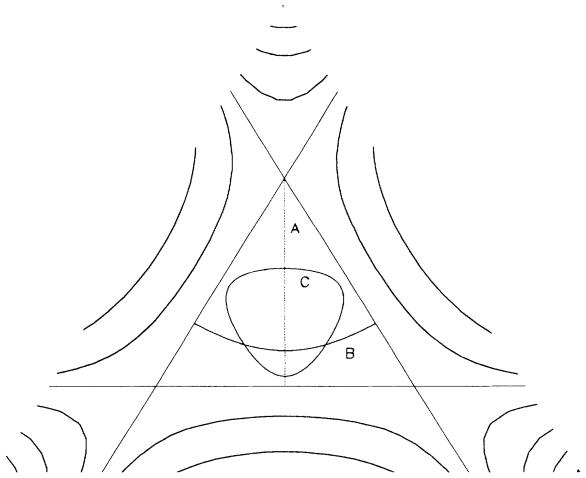

FIG. 1. The Hénon-Heiles equipotentials outside the triangle defined by $E = E^*$. The three classical periodic orbits of shortest lengths A ("linear"), B ("smiley"), and C ("loop") are displayed for $E = E^*$.

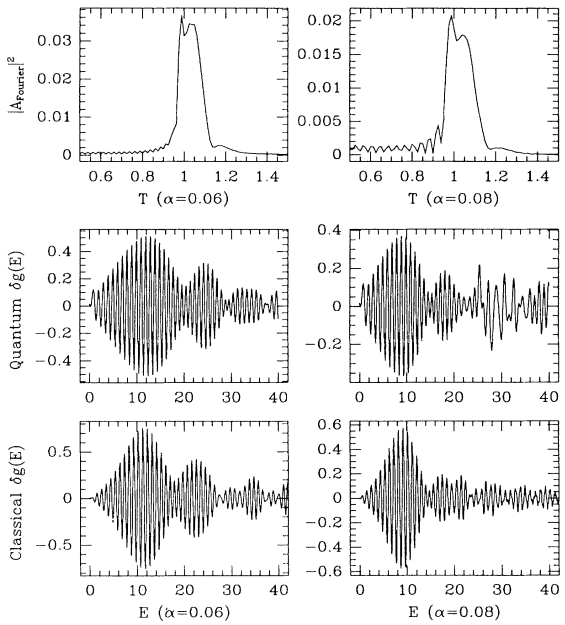

FIG. 2. Middle row: Oscillating part $\delta g(E)$ of the quantum density of states for the Hénon-Heiles Hamiltonian. Top row: Fourier transform of the quantum $\delta g(E)$. Bottom row: Result of the classical periodic orbit calculation of $\delta g(E)$, Eq. (4). Left column: $\alpha = 0.06$. Right column: $\alpha = 0.08$.

The density of states $g(E) = \sum_i \delta(E - E_i)$ of a quantum system is well known to have a smooth part (the "Thomas-Fermi part"), and an oscillating part that gives rise to shell effects [6, 15, 16]. The smooth part may be obtained from the semiclassical partition function [17] or the equivalent Green's function [18]. The oscillating part may be approximated [1, 6] by a sum over all periodic orbits of the classical system. In this work, we obtain the smooth part of the level density by the Strutinsky averaging procedure [16, 19]. This consists in replacing each delta function $\delta(E - E_i)$ by some smoothing function of half-width $\tilde{\gamma}$, usually taken to be a Gaussian, with appropriate curvature-correction terms. Effectively, a smoothing parameter $\tilde{\gamma}$ equal to or slightly larger than the main-shell spacing in the spectrum E_i (i.e., $\hbar\omega$ for a harmonic oscillator) wipes out all the oscillations in $g(E)$, and only the average part survives which in simple model potentials is identical to the (extended) Thomas-Fermi level density [17, 19]. Following Strutinsky [16], we define the oscillating part of the level density by

$$\delta g(E) = [g_{\gamma_{\rm osc}}(E) - g_{\tilde{\gamma}}(E)]. \qquad (2)$$

Hereby we use a finite smoothing parameter $\gamma_{\rm osc}$ to damp the δ functions in the exact $g(E)$. We choose the values [20] $\gamma_{\rm osc} = 0.6$ and $\tilde{\gamma} = 1.2$. Generally, $\gamma_{\rm osc}$ may be used as a filter for studying the effects of different harmonics in $\delta g(E)$. With the present value, the quantity $\delta g(E)$ contains only the fundamentals, corresponding to the shortest periods, and possible beats. All higher harmonics are suppressed [21]. Note, however, that the overall magnitude of $\delta g(E)$ depends on the choice of $\gamma_{\rm osc}$, since it tends to vanish as $\gamma_{\rm osc} \to \tilde{\gamma}$.

The $\delta g(E)$ obtained from the Hénon-Heiles quantum spectrum is shown in the middle row of Fig. 2 for $\alpha = 0.06$ and $\alpha = 0.08$ and exhibits prominent beats. A discrete fast Fourier transform (FFT) gives the results shown in the top row of Fig. 2. For the Fourier analysis at $\alpha = 0.06$ the entire energy range $0 \le E \le 40$ was chosen, whereas for $\alpha = 0.08$ the energy cutoff was taken at $E = E^* = 26$, since beyond the saddle point energy E^* the quantum spectrum appears to be less reliable, judging from its rather irregular behavior. The abscissas of the Fourier spectra show the time scale with T=1 corresponding to the period of the unperturbed harmonic oscillator. The spectrum at $\alpha = 0.06$ reveals one period slightly below 1 and two others slightly above 1. The same pattern is repeated for $\alpha = 0.08$. In the latter case, the higher peak is not resolved [22] and from the Fourier spectrum alone it is not clear if it contains two distinct periods. However, it does show that the amplitudes of the leading components are quite comparable. We shall in the following interpret all these features in a discussion of the periodic orbits of the classical system.

In Fig. 1, the well-known Hénon-Heiles equipotentials are displayed. Solving the classical equations of motion numerically, we found for $E < E^*$ three distinct classes of periodic orbits, shown in Fig. 1, which we labeled A ("saddle mode"), B ("smiley" mode), and C ("loop"). Orbits A and B occur in three orientations according to the symmetry of the potential. These three orbits are the ones with the smallest periods, close to the oscillator

period ($T = 1$), for low E. Here, the orbits A and C are stable, while orbit B is always unstable. As E approaches the threshold E^*, the situation becomes more complicated; A does not exist beyond E^* (where its period diverges), whereas B and C can be found also well above E^*, although being unstable there [23].

In the Hamiltonian (1), the strength parameter α may be scaled away by defining new scaled variables $\xi = \alpha x, \eta = \alpha y$. Then the classical equations of motion in the variables ξ, η no longer depend explicitly on α. The motion is thus "universal" in these coordinates, with a scaled energy $\alpha^2 E$. It is sufficient to solve the equations of motion once for each value of $\alpha^2 E$. In terms of the dimensionless energy variable $e = E/E^* = 6\alpha^2 E$, we have parametrized the numerically obtained actions S of the above three primitive orbits by

$$\begin{aligned} S_{\rm A}(e,\alpha) &= (2\pi/6\alpha^2)(e + 0.09e^2 + 0.056e^6) \quad (0 \le e \le 1), \\ S_{\rm B}(e,\alpha) &= (2\pi/6\alpha^2)(1.02e + 0.044e^2) \quad (0 \le e \le 2), \\ S_{\rm C}(e,\alpha) &= (2\pi/6\alpha^2)(0.98e - 0.025e^4) \quad (0 \le e \le 2). \end{aligned} \tag{3}$$

These fits reproduce the numerical results within $< 3\%$ in the energy regions shown. [Note that one finds analytically $S_{\rm A}(e=1) = S_{\rm A}^* = 6/5\alpha^2 = 1.146\ (2\pi E^*)$.] The classical periods, obtained by $T_q = \partial S_q/\partial E$, agree with the Fourier spectra shown in the top row of Fig. 2, after averaging them over the energy interval used for the FFT. Indeed, we see from Eq. (3) that one averaged period (C) is slightly below $T = 1$ and the other two are slightly above 1. Because of their different energy dependence, the Fourier analysis cannot give clean signals but only averaged periods. Therefore the two higher periods (A and B) could not be resolved better in the Fourier spectra.

We anticipate that these periodic orbits yield $\delta g(E)$ classically through the Gutzwiller trace formula. Since we have smoothed out the higher harmonics of the quantum $\delta g(E)$, we only take the lowest harmonics. Superposing the contributions of the above three orbits, we write

$$\delta g_{\rm cl}(E) = \Big[\ \mathcal{A}_{\rm A}\cos(S_{\rm A} - \pi) + \mathcal{A}_{\rm B}\cos(S_B - \pi) + 2\mathcal{A}_{\rm C}\cos(S_{\rm C})\Big]. \tag{4}$$

Here $\mathcal{A}_q(E)$ are the amplitudes obtained from the periods and the relevant eigenvalues of the monodromy matrix for the corresponding orbits (q =A,B,C), and $S_q(E)$ are the actions given in Eq. (3) above. The extra factor 2 for the "loop" contribution (C) takes into account the two orientations of orbiting. We have used the numerical monodromy method introduced by Baranger, Davies, and Mahoney [24].

In Fig. 3 we show the calculated amplitudes $\mathcal{A}_q$ as functions of energy. It might come as a surprise that the amplitude of the "smiley" orbit B, although unstable throughout, is found to be larger than that of the "loop" orbit C which is stable up to $e \sim 0.89$. Note that the amplitudes for A and B are very close up to $e \sim 0.9$, beyond which $\mathcal{A}_{\rm A}$ diverges repeatedly (see the reference quoted in [23]). For $e > 1$, of course, $\mathcal{A}_{\rm A} = 0$; there the amplitude of the "loop" mode C becomes close to that of the "smiley" mode B.

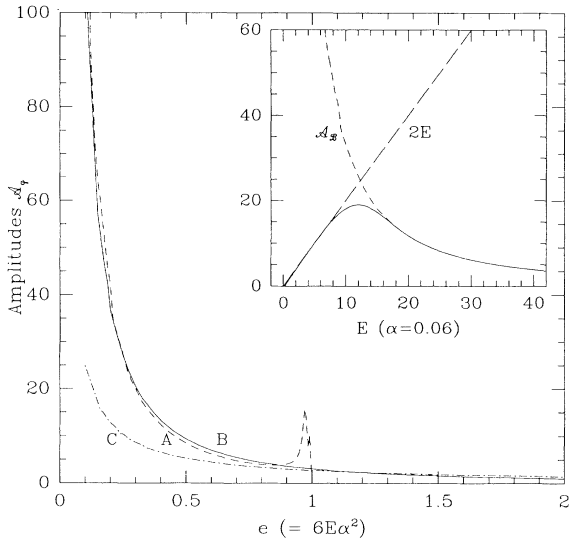

FIG. 3. Amplitudes $\mathcal{A}_q$ of the Hénon-Heiles orbits A (dashed line; does not exist for $e > 1$), B (solid line), and C (dot-dashed line) in Gutzwiller's trace formula, as obtained numerically from the monodromy matrix. Inset: Exact harmonic-oscillator amplitude $2E$, common to all orbits (dashed straight line), and amplitude $\mathcal{A}_{\rm B}$ of orbit B in the Hénon-Heiles potential (short-dashed line). The solid line shows a spline fit connecting the exact numerical amplitude for $E > 16$ to its oscillator limit $2E$ for $E < 8$. This splined amplitude $\mathcal{A}_{\rm B}$ is used in Eq. (4); the amplitudes $\mathcal{A}_{\rm A}$ and $\mathcal{A}_{\rm C}$ are obtained from the ratios of the numerically obtained values of $\mathcal{A}_q$ in the whole energy domain.

For low energies, the harmonic part of the Hénon-Heiles potential dominates, and the trace of the monodromy matrix is close to 4. This leads to the well-known breakdown of the Gutzwiller trace formula; the amplitudes thus diverge when $E \to 0$. In order to salvage the method, we note that for an isotropic two-dimensional harmonic oscillator, the quantum $\delta g(E)$ is exactly given [25] by $\delta g(E) = 2E\sum_{n=1}^{\infty}\cos(2\pi nE)$. From this we infer that the correct amplitudes in the trace formula should, in the limit $E \to 0$, all approach $2E$. We impose this by hand, as shown by the inset in Fig. 3 for the orbit B which we take as a reference. The other two amplitudes are obtained from the ratios of the calculated monodromy amplitudes. This procedure is somewhat arbitrary but ensures that Eq. (4) can be applied also for small E.

The resulting $\delta g_{\rm cl}(E)$ is shown in the bottom row of Fig. 2. It is seen to reproduce the main features of the

quantum $\delta g(E)$ rather well. For energies around and above the threshold E^*, many more isolated periodic orbits can be found (e.g., also a stable double-loop orbit), which will contribute to $\delta g(E)$. We have not attempted to enumerate and calculate their amplitudes, since our quantum spectrum is only approximate for $E > E^*$ due to the neglect of the imaginary parts of the eigenenergies [cf. the irregular behavior of $\delta g(E)$ for $\alpha = 0.08$ above $E^* = 26$ in Fig. 2].

In conclusion, we have demonstrated the existence of quantum beats in a system that is classically chaotic. The beats are shown to originate, using the approach of Gutzwiller, from the interference of three simple classical orbits of comparable periods and amplitudes, that are partially stable and partially unstable. This novel feature in the spectral density introduces a long-range correlation in the energy scale which coexists with the short-range correlations connected to the chaotic behavior of the system.

It has not escaped our notice that back in 1964, the same form of a potential in deformation space was used [26] to study the collective states of nonaxial atomic nuclei. Indeed, recent calculations show chaotic signatures in the collective spectrum of such nuclei [27].

This research was supported by the Natural Sciences and Engineering Research Council of Canada, and in part (M.B.) by Deutsche Forschungsgemeinschaft. We have profited from discussions with D. Goodings, H. Nishioka, T. Szeredi, J. Waddington, and Hua Wu. We thank Hema Murthy for her invaluable assistance in the Fourier analysis. M.B. and M.V.N. acknowledge the hospitality of the Department of Physics and Astronomy at McMaster, and M.B. and R.K.B. that of the Institute of Mathematical Sciences at Madras.

[1] M. C. Gutzwiller, *Chaos in Classical and Quantum Mechanics* (Springer-Verlag, New York, 1990); J. Math. Phys. **10**, 1004 (1969); **11**, 1791 (1970); **12**, 343 (1971).
[2] M. Berry, in *Chaos and Quantum Physics*, Proceeding of the Les Houches Summer School Session LII, edited by M. J. Giannoni, A. Voros, and J. Zinn-Justin (Elsevier, Amsterdam, 1991), p. 252.
[3] S. W. McDonald and A. N. Kaufman, Phys. Rev. Lett. **42**, 1189 (1979).
[4] O. Bohigas, M. J. Giannoni, and C. Schmit, Phys. Rev. Lett. **52**, 1 (1984).
[5] T. Ericson, Adv. Phys. **9**, 425 (1960).
[6] M. C. Gutzwiller, J. Math. Phys. **8**, 1979 (1967).
[7] D. Wintgen, Phys. Rev. Lett. **58**, 1589 (1987).
[8] R. Balian and C. Bloch, Ann. Phys. (N.Y.) **69**, 76 (1972).
[9] H. Nishioka, K. Hansen, and B. R. Mottelson, Phys. Rev. B **42**, 9377 (1990).
[10] J. Pedersen, S. Bjørnholm, J. Borggreen, K. Hansen, T. P. Martin, and H. D. Rasmussen, Nature (London) **353**, 733 (1991).
[11] M. Hénon and C. Heiles, Astrophys. J. **69**, 73 (1964).
[12] R. C. Churchill, G. Pecelli, and D. L. Rod, in *Stochastic Behaviour in Classical and Quantum Hamiltonian Systems*, edited by G. Casati and J. Ford (Springer-Verlag, New York, 1979), p. 76.
[13] N. Pomphrey, J. Phys. B **7**, 1909 (1974); D. W. Noid and R. A. Marcus, J. Chem. Phys. **67**, 559 (1977); D. W. Noid, M. L. Koszykowski, M. Tabor, and R. A. Marcus, J. Chem. Phys. **72**, 6169 (1980); R. A. Pullen and A. R. Edmonds, J. Phys. A **14**, L319 (1981).
[14] C. K. Ross and R. K. Bhaduri, Nucl. Phys. **A188**, 566 (1972).
[15] W. D. Myers and W. J. Swiatecki, Nucl. Phys. **81**, 1 (1966).
[16] V. M. Strutinsky, Yad. Fiz. **3**, 614 (1966) [Sov. J. Nucl. Phys. **3**, 449 (1966)]; Nucl. Phys. **A95**, 420 (1967); **A122**, 1 (1968).
[17] R. K. Bhaduri and C. K. Ross, Phys. Rev. Lett. **27**, 606 (1971); B. K. Jennings, Ann. Phys. (N.Y.) **84**, 1 (1974).
[18] R. Balian and C. Bloch, Ann. Phys. (N.Y.) **60**, 401 (1970); **64**, 271 (1971).
[19] M. Brack and H. C. Pauli, Nucl. Phys. **A207**, 401 (1973).
[20] A second-order curvature correction suffices here for the smoothing with $\tilde{\gamma}$ to fulfil the "plateau condition" [19]; no correction is included in the smoothing with $\gamma_{\rm osc}$.
[21] Compare also C. P. Malta and A. M. Ozorio de Almeida, J. Phys. A **23**, 4137 (1990), who used a similar analysis for different nonlinear potentials.
[22] The resolution in the time domain depends on the energy range of the given "signal" $\delta g(E)$. We artificially doubled the energy interval, putting a null signal in the upper half interval.
[23] After the submission of our paper, the work of K. T. R. Davies, T. E. Huston, and M. Baranger, Chaos **2**, 215 (1992), has appeared. They give an exhaustive discussion of many classical orbits in the Hénon-Heiles potential and their regions of stability.
[24] M. Baranger, K. T. R. Davies, and J. H. Mahoney, Ann. Phys. (N.Y.) **186**, 95 (1988).
[25] R. K. Bhaduri and B. K. Jennings (unpublished); see also V. M. Strutinsky, A. G. Magner, S. R. Ofengenden, and T. Døssing, Z. Phys. A **283**, 269 (1977); and A. G. Magner, Yad. Fiz. **28**, 1477 (1978) [Sov. J. Nucl. Phys. **28**, 759 (1978)], for the semiclassical treatment of the three-dimensional harmonic oscillator.
[26] S. Das Gupta and M. R. Gunye, Can. J. Phys. **42**, 1822 (1964).
[27] Y. Alhassid, A. Novoselsky, and N. Whelan, Phys. Rev. Lett. **65**, 2971 (1990).